

Temperature and spatial diffusion of atoms cooled in a 3D lin⊥lin bright optical lattice

F.-R. Carminati, M. Schiavoni, L. Sanchez-Palencia, F. Renzoni and G. Grynberg

Laboratoire Kastler-Brossel, Département de Physique de l'École Normale Supérieure, 24 rue Lhomond, 75231, Paris Cedex 05, France

(October 22, 2018)

We present a detailed experimental study of a three-dimensional lin⊥lin bright optical lattice. Measurements of the atomic temperature and spatial diffusion coefficients are reported for different angles between the lattice beams, i.e. for different lattice constants. The experimental findings are interpreted with the help of numerical simulations. In particular we show, both experimentally and theoretically, that the temperature is independent of the lattice constant.

32.80.Pj, 42.65.Dr, 42.65.Es

I. INTRODUCTION

The spatial modulation of the intensity or polarization of laser beams leads to cooling and trapping of atoms [1,2]. In the case of a *periodic* spatial modulation of the light, the trapping of atoms results in their localization in a periodic structure, called optical lattice [3,4].

Near-resonant bright optical lattices, the ones considered in this work, are based on the Sisyphus cooling mechanism [2,5]. The periodic modulation of the light polarization, produced by the interference of several laser beams, leads to a periodic modulation of the light shifts (optical potentials) of the different Zeeman sublevels of the ground state of the atom. As a result of the optical pumping between different optical potentials, atoms are cooled and finally trapped at the potential minima.

The lin⊥lin configuration, which corresponds to a Sisyphus cooling, and the $\sigma^+ - \sigma^-$ one have been the first laser cooling schemes leading to sub-Doppler temperatures [2]. Therefore much experimental and theoretical work has been done on these cooling schemes, and many temperature measurements have been reported. However the majority of the experimental data corresponds to 1D configurations or to 3D optical molasses produced by six phase-uncontrolled laser beams [6]. A much smaller amount of experimental data is available for 3D optical lattices, as obtained by the interference of four phase-uncontrolled laser beams [7]. Besides the early studies by our group [4], temperature measurements for a four-beam 3D lattice have been done at NIST [8] and later on by the Kastberg's group [9,10]. In these works the temperature of the atoms in a lattice with fixed geometry was studied as a function of the atom-light interaction parameters (laser intensity and detuning, corresponding to different depths of the potential well and different optical pumping rates). No attention was paid to depen-

dencies of the temperature on geometrical parameters as the lattice constants, which can be varied by changing the angles between the lattice beams. That is one of the issues analyzed in the present work.

Another aspect of optical lattices relatively unexplored is the diffusive atomic dynamics. That will be the second issue analyzed in this work. In a bright optical lattice, as obtained with a laser field red detuned from a $F_g = F \rightarrow F_e = F + 1$ transition, atoms at the bottom of a potential well strongly interact with the light and therefore undergo fluorescence cycles. This produces complex transport phenomena which have not yet been completely understood. Two different mechanisms may lead to spatial diffusion. First, the optical pumping may transfer an atom from a potential well to a neighbouring one corresponding to a different optical potential, as shown in Fig. 1. Second, atoms are heated as result of the recoil associated to the fluorescence cycles. Thus, the increase in kinetic energy following many fluorescence cycles may allow the atom to leave the potential well. In this case the atomic diffusion is not associated to optical pumping between different ground state sublevels.

There has already been a few investigations devoted to the study of spatial diffusion in optical molasses and bright optical lattices [11–15]. In Refs. [11–14] the atomic transport and spatial diffusion has been studied by a direct imaging of the expansion of the atomic cloud. A completely different approach has been followed in Ref. [15] where both the atomic dynamics in a single potential well and the atomic transport in the lattice have been studied through polarization-selective intensity correlation spectroscopy.

In this work we present a detailed experimental study of the temperature and spatial diffusion of ^{85}Rb atoms cooled in a 3D lin⊥lin bright optical lattice. Measurements for different angles between the lattice beams, i.e. for different lattice constants, are presented. The experimental results are compared with numerical simulations.

This work is organized as follows. In Section II we describe the experimental set-up. Section III contains the results of the temperature measurements obtained by recoil-induced resonances and the corresponding numerically calculated values. In Section IV we present our results for the measurement of the spatial diffusion coefficients by direct imaging of the atomic cloud and we compare them with the numerical simulations. Finally, in Section V we present the conclusions of our work.

II. EXPERIMENTAL SET-UP

The preparation of the atoms in the optical lattice is the standard one used in previous experiments [7]. The rubidium atoms are cooled and trapped in a magneto-optical trap (MOT). Then the MOT magnetic field and laser beams are turned off and the atoms are cooled and trapped in the optical lattice. The periodic structure is determined by the interference of four linearly polarized laser beams, arranged as shown in Fig. 2: two y -polarized beams, symmetrically disposed with respect to the z axis, propagate in the xOz plane with a relative angle $2\theta_x$, while two x -polarized beams, also symmetrically disposed with respect to the z axis, propagate in the yOz plane and form an angle $2\theta_y$. As discussed in Refs. [7,16], this configuration results in a 3D periodic potential, with minima located on an orthorhombic lattice and associated with pure circular (alternatively σ^+ and σ^-) polarization.

For the measurements presented in this work, the angles between the lattice beams in the xOz and yOz planes are equal: $\theta_x = \theta_y \equiv \theta$. This corresponds to the lattice constants, i.e. to the distance (along a major axis) between two sites of equal circular polarization, $\lambda_{x,y} = \lambda/\sin\theta$, $\lambda_z = \lambda/(2\cos\theta)$, with λ the laser field wavelength. For this configuration with equal angles and equal intensity laser beams the radiation pressure is balanced.

For the MOT and the lattice we used the $F_g = 3 \rightarrow F_e = 4$ D₂ line transition of ⁸⁵Rb. A repumping beam resonant to the $F_g = 2 \rightarrow F_e = 3$ transition is also added.

III. TEMPERATURE MEASUREMENTS

We measured the temperature of the atomic sample after a 20 ms cooling phase in the optical lattice by using the method of recoil-induced resonances [17–19]. Once the lattice beams are turned off, two additional laser beams (the pump and the probe beams, see Fig. 2) are introduced for the temperature measurements. They cross the atomic sample in the xOz plane, and they are symmetrically disposed with respect to the z axis forming an angle of 23° . The probe transmission is monitored as a function of the detuning between the pump and probe fields. For equal pump and probe polarizations, the states $|\alpha, p\rangle$ and $|\alpha, p'\rangle$ with the same internal quantum number α but different atomic momentum are coupled by Raman transitions. The difference in population of these states determines the absorption or gain of the probe, and the probe transmission spectrum results to be proportional to the derivative of the atomic momentum distribution. From the width of the resonance in the probe transmission spectrum it is then straightforward to derive the atomic temperature [18]. The geometry of our pump and probe fields corresponds to measurement of the temperature in the x direction [20].

Results of our measurements for the temperature as a function of the lattice beam intensity at different values of the lattice detuning and for different choices of the lattice angle θ are shown in Fig. 3.

We observe a linear dependence of the temperature with the laser intensity, with a *décrochage* at small intensities, in agreement with theoretical models and previous measurements [9,10].

As an original result, on the basis of the measurement reported in Fig. 3, we find that the temperature is independent of the angle between the lattice beams, i.e. of the lattice constant. However, this behaviour, independent of the lattice constant, is specific of the temperature and we should not conclude that the atomic dynamics does not depend on the lattice constants. In fact, as we will show in the following, other quantities, such as the spatial diffusion coefficients, show a strong dependence on the angle between the lattice beams.

We also studied the temperature of the atomic sample as a function of the lattice detuning Δ , for different depths of the potential well U_0 , i.e. for different values of the light shift per beam Δ'_0 (U_0 is proportional to Δ'_0). Results of our measurements are shown in Fig. 4. We conclude that the temperature depends on the depth of the potential well only, and not on the lattice detuning, except for an increase at small detunings. We have also performed a theoretical study with the help of semi-classical Monte Carlo simulations [21]. Taking advantage of the symmetry between the x and y directions (see Fig. 2), we restricted the atomic dynamics in the xOz plane. The numerical calculations in this restricted configuration give the same dependencies of the dynamical quantities on the lattice parameters as full 3D calculations, so they are useful to interpret the experimental results. However, a direct quantitative comparison is not necessarily meaningful because the restriction of the dynamics to two dimensions may introduce scaling factors (see [21] for more details).

We considered $1/2 \rightarrow 3/2$ atoms, as customary in numerical analyses of Sisyphus cooling. Because the external degrees of freedom of the atoms are treated as classical variables, it is straightforward to calculate the variance of the atomic momentum distribution, which is proportional to the steady-state temperature in a thermalized cloud

$$k_B T_i = \frac{\langle p_i^2 \rangle}{M} \quad (i = x, z), \quad (1)$$

with p_i the atomic momentum in the i -direction, M the atomic mass and k_B the Boltzmann constant. We found results in good agreement with the experimental ones. In particular, the independence of the temperature on the lattice angle is well confirmed by the numerical simulations. The physical picture of Sisyphus cooling [2] allows an immediate interpretation of this result: an atom loses kinetic energy until it gets smaller than the depth of the potential well, independently of the lattice

constant. More precisely in the regime considered here (the *jumping* regime [2]), the atomic dynamics is well described by a brownian motion: an atom undergoes a friction force $F_i = -\alpha_i v_i$ and a fluctuating force, essentially produced by the fluctuations of the dipole force, which is described by the momentum diffusion coefficient D_{p_i} in the i - direction. As shown in Ref. [21], α_i and D_{p_i} are proportional to $1/\lambda_i^2$ in a domain where the spontaneous emission can be neglected. Hence, the temperature, given by the Einstein relation $k_B T_i = D_{p_i}/\alpha_i$, is independent of the lattice constants.

The increase of the temperature at small lattice detuning is also present in our numerical results. As the laser frequency gets close to the atomic resonance the momentum diffusion corresponding to multiple atomic recoils increases while the friction coefficient associated to the Sisyphus cooling decreases [2]. As a result, at small lattice detuning the equilibrium temperature increases approaching the atomic resonance. We verified this point by arbitrarily removing the corresponding term in the simulation. Then, no increase of the temperature at small detuning appeared.

IV. MEASUREMENT OF THE SPATIAL DIFFUSION COEFFICIENTS

We now turn to the study of spatial diffusion. We observed the atomic cloud expansion by using a Charge Coupled Device (CCD) camera. We took images of the expanding cloud at different instants after the atoms have been loaded into the optical lattice. The exposure lasts 1 ms and we took an image every 7 ms. Since we wanted to explore regions of large detuning and low intensity for the lattice beams, we increased to maximum the lattice beams intensity while imaging the atomic cloud to increase the brightness of the image. Of course, the atomic dynamics was affected during the imaging and we took only an image for every realization of the diffusion. Since the x and y directions are equivalent in our lattice, we choose to take images in a plane containing the z axis and forming an angle of 45° with the x and y axis (ξ axis). Fig. 5 shows typical images of the expanding cloud.

We verified that the profile of the atomic cloud is well approximated by a gaussian function (Fig. 5, right). From the images of the atomic cloud we derived the atomic mean square displacements $\langle \Delta z^2 \rangle$ and $\langle \Delta \xi^2 \rangle$. As evidenced by the plots of Fig. 6, the cloud expansion corresponds to a normal diffusion, i.e. the mean square atomic displacement increases linearly with time.

From data as those of Fig. 6 we have been able to derive the spatial diffusion coefficients D_z and D_ξ in the z - and ξ -directions by fitting the experimental data with

$$\langle \Delta x_i^2 \rangle = 2D_i t \quad (i = z, \xi) . \quad (2)$$

We determined the spatial diffusion coefficients as a function of the lattice beam intensity for different values of

the laser detuning and lattice constant. Our results are shown in Fig. 7.

It appears that D_ξ is an increasing function of the lattice intensity. On the other hand, the experimental data do not show a clear general dependence of D_z on the laser intensity.

As an important fact, we observe that D_ξ is a decreasing function of the angle θ between the lattice beams. This supports the picture of the atomic spatial diffusion as produced by optical pumping (see Fig. 1). Indeed if we assume that the diffusion is produced by the optical pumping between neighbouring wells, the diffusion coefficients (Eq. 2) will be simply proportional to the pumping rate and to the square of the lattice constant. As the lattice constant $\lambda_{x,y} = \lambda/\sin\theta$ decreases for increasing θ , the spatial diffusion coefficients decreases as a result.

It is difficult to test whether a similar argument applies also to the diffusion in the z direction, as the range of $\lambda_z = \lambda/(2\cos\theta)$ explored experimentally has been quite small because of practical difficulties with lattice beams with very large or very small angles. However we note that at large lattice intensity, the spatial diffusion coefficient in the z - direction increases for increasing λ_z , i.e. for increasing θ , as expected. This behaviour is not observed at small lattice intensity.

In the numerical simulations, we monitored the variance of the atomic position distribution as a function of time. We verified that the spatial diffusion is normal, and determined the diffusion coefficients from Eq. 2. The results of our calculations are shown in Fig. 8.

We note a linear dependence of the diffusion coefficients on the lattice beams intensity, and a *décrochage* at small intensity. For the values of lattice intensity at which this *décrochage* is observed, the temperature is still in the linear regime (T proportional to Δ_0). This corresponds to a transition to anomalous diffusion [22], where only few atoms, flying over several potential wells, contribute to the diffusion process.

In the linear regime, D_i is proportional to λ_i^2 ($i = \xi, z$), in agreement with the simple picture presented above and with the experimental results along the ξ axis. On the contrary, in the regime of *décrochage*, the atoms do not move from a well to a neighbouring one so no variation of D_i proportional to λ_i^2 is expected. Both the experimental and theoretical results confirm that D_i is not proportional to λ_i^2 in this regime.

V. CONCLUSIONS

In conclusion, we studied, experimentally and theoretically, the temperature and the spatial diffusion of rubidium atoms cooled in a 3D lin \perp lin optical lattice. The atomic temperature and the spatial diffusion coefficients are studied for different angles between the lattice beams, i.e. for different lattice constants. The experimental find-

ings are interpreted with the help of numerical simulations.

We show, both experimentally and theoretically, that the temperature is independent of the lattice constants. This is consistent with a simple physical picture: an atom loses kinetic energy until it gets smaller than the depth of the potential well, independently of the lattice constants.

The experimental results for the spatial diffusion coefficients show a linear dependence on the lattice beams intensity, and a *décrochage* at small intensity. Both *décrochage* and linear regime are confirmed by the numerical simulations. However in the experiment the *décrochage* in the different directions does not appear at the same values of lattice parameters, in contrast with the theoretical predictions. We have not been able to determine with certainty the origin of this discrepancy. The choice of the $1/2 \rightarrow 3/2$ transition for the numerical simulations, different from the one of the experiment, could be a source of disagreement between the theoretical results and the experimental findings. This point requires further analysis.

In the linear regime, the numerical simulations show that the spatial diffusion coefficient is proportional to the square of the lattice constant, in agreement with the picture of atomic diffusion produced by optical pumping. Experimental findings for the diffusion coefficients along the ξ axis and also along the z axis for much higher intensities that that leading to *décrochage* confirm the theoretical predictions.

We are grateful to Franck Laloë for his continuous interest in our work. We also wish to thank C. Mennerat-Robilliard and S. Guibal for fruitful discussions. This work was supported by the European Commission (TMR network "Quantum Structures", contract FMRX-CT96-0077). Laboratoire Kastler Brossel is an "unité mixte de recherche de l'École Normale Supérieure et de l'Université Pierre et Marie Curie associée au Centre National de la Recherche Scientifique (CNRS)".

-
- [1] R. Grimm, M. Weidemüller, and Yu.B. Ovchinnikov, *Adv. At. Mol. Opt. Phys.* **42**, 95 (2000).
 - [2] J. Dalibard and C. Cohen-Tannoudji, *J. Opt. Soc. Am. B* **6**, 2023 (1989); P.J. Ungar, D.S. Weiss, E. Riis and S. Chu, *ibid* **6**, 2058 (1989).
 - [3] P.S. Jessen and I.H. Deutsch, *Adv. At. Mol. Opt. Phys.* **37**, 95 (1996).
 - [4] C. Mennerat-Robilliard and G. Grynberg, *Phys. Rep.*, (2001) in press.
 - [5] Y. Castin and J. Dalibard, *Europhys. Lett.* **14**, 761 (1991).
 - [6] For a review of laser cooling, see H.J. Metcalf and P. van der Straten, *Laser cooling and trapping*, Springer-Verlag

(Berlin, 1999).

- [7] P. Verkerk, D.R. Meacher, A.B. Coates, J.-Y. Courtois, S. Guibal, C. Salomon and G. Grynberg, *Europhys. Lett.* **26**, 171 (1994).
- [8] M. Gatzke, G. Birkl, P.S. Jessen, A. Kastberg, S.L. Rolston and W.D. Phillips, *Phys. Rev A* **55**, R3987 (1997).
- [9] J. Jersblad, H. Ellmann, and A. Kastberg, *Phys. Rev. A* **62**, 051401 (2000).
- [10] H. Ellmann, J. Jersblad, and A. Kastberg, *Eur. Phys. J. D* **13**, 379 (2001).
- [11] T.W. Hodapp, C. Gerz, C. Furtlehner, C.I. Westbrook, W.D. Phillips, J. Dalibard, *Appl. Phys. B.* **60**, 135 (1995).
- [12] C. Mennerat-Robilliard, D. Boiron, J.M. Fournier, A. Aradian, P. Horak and G. Grynberg, *Europhys. Lett.* **44**, 442 (1998).
- [13] G. Grynberg, P. Horak and C. Mennerat-Robilliard, *Europhys. Lett.* **49**, 424 (2000).
- [14] L. Guidoni, B. Dépret, A. di Stefano, and P. Verkerk, *Phys. Rev. A* **60**, R4233 (1999).
- [15] C. Jurczak, B. Desruelle, K. Sengstock, J.-Y. Courtois, C.I. Westbrook and A. Aspect, *Phys. Rev. Lett.* **77**, 1727 (1996).
- [16] K.I. Petsas, A.B. Coates, and G. Grynberg, *Phys. Rev. A* **50**, 5173 (1994).
- [17] J.-Y. Courtois, G. Grynberg, B. Lounis and P. Verkerk, *Phys. Rev. Lett.* **72**, 3017 (1994).
- [18] D.R. Meacher, D. Boiron, H. Metcalf, C. Salomon and G. Grynberg, *Phys. Rev. A* **50**, R1992 (1994).
- [19] J.-Y. Courtois and G. Grynberg, *Adv. At. Mol. Opt. Phys.* **36**, 87 (1996).
- [20] We note that the temperature in z direction can be different from the ones in the (equivalent) x and y directions. In fact, as it will be discussed in detail in the following, the temperature depends on the depth of the potential well. Therefore in the case of anisotropy of the optical potentials, the temperatures in the different directions are different.
- [21] A complete account of the theoretical work will be given in L. Sanchez-Palencia, P. Horak and G. Grynberg, to be published. There, also regimes non relevant for the present experimental study will be examined.
- [22] S. Marksteiner, K. Ellinger and P. Zoller, *Phys. Rev. A* **53**, 3409 (1996).

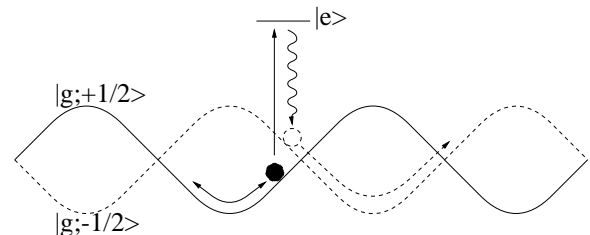


FIG. 1. Process of spatial diffusion produced by optical pumping between different optical potentials. The shown potentials correspond to a $J_g = 1/2 \rightarrow J_e = 3/2$ transition in counterpropagating laser fields with orthogonal linear polarizations.

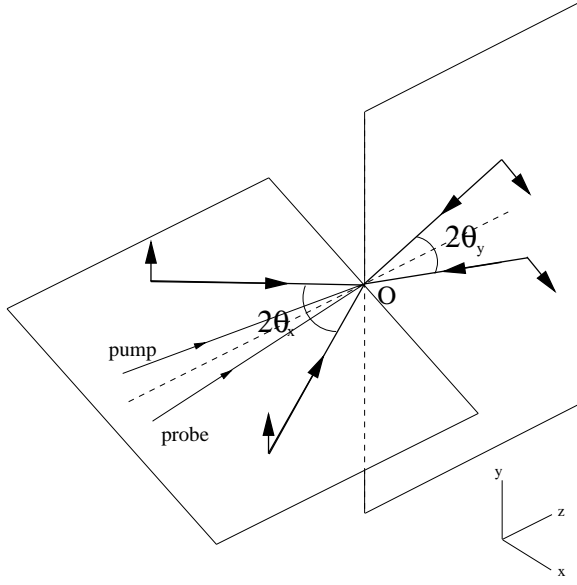


FIG. 2. Sketch of the experimental setup. We indicate by $2\theta_x$ ($2\theta_y$) the angle between the lattice beams in the xOz (yOz) plane. For the measurements presented in this work, the angles between the lattice beams in the xOz and yOz planes are equal: $\theta_x = \theta_y \equiv \theta$. Two additional laser fields (the pump and probe beams) are used for the temperature measurements.

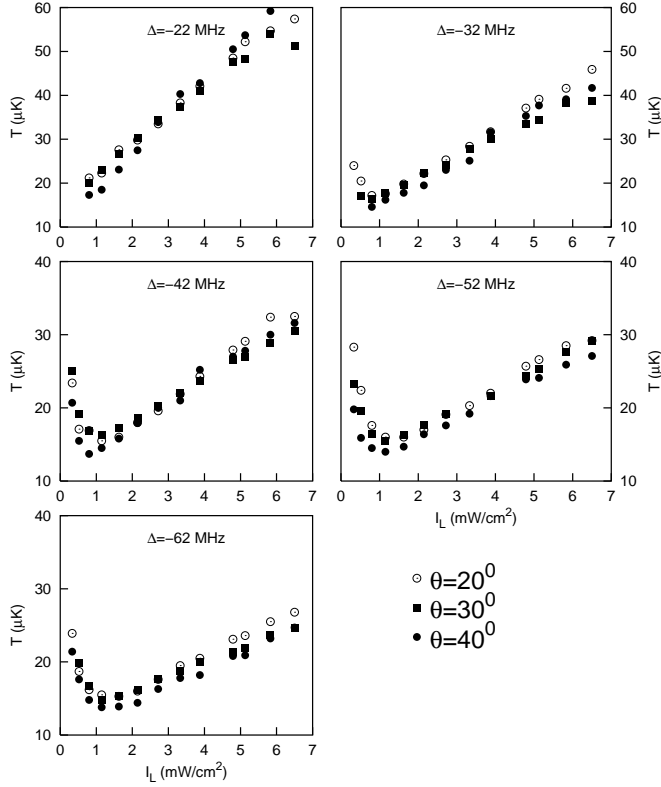


FIG. 3. Atomic temperature in the x direction as a function of the intensity per lattice beam I_L at different values of the lattice detuning Δ and for different choices of the lattice angle θ .

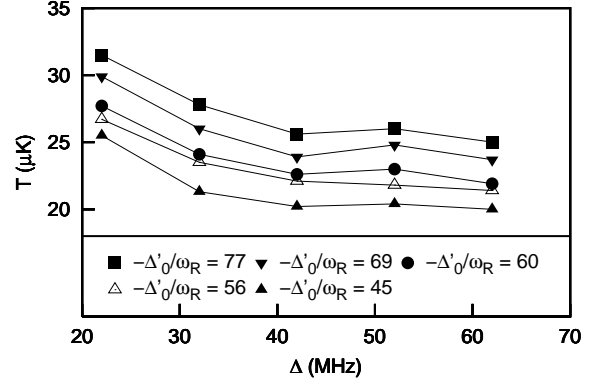


FIG. 4. Atomic temperature in the x direction as a function of the lattice detuning Δ , for different values of the light shift per beam Δ'_0 , *i.e.* at different depths of the potential well (ω_R is the atomic recoil frequency). The data refer to a lattice angle $\theta = 30^\circ$. The lines are guides for the eyes.

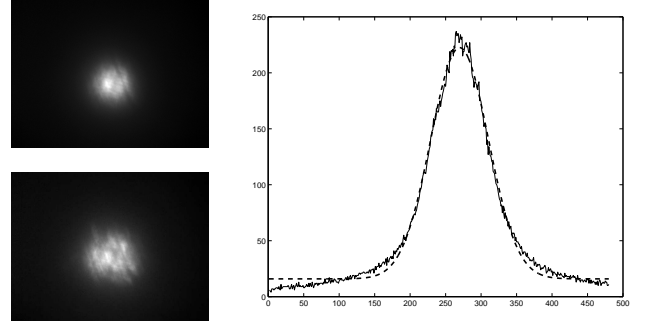


FIG. 5. Left: Images of the atomic cloud after 50 *ms* (top) and 400 *ms* (bottom) from the loading of the optical lattice. Right: A typical profile of the atomic cloud (continuous line). The dashed line represents the best fit with a gaussian function.

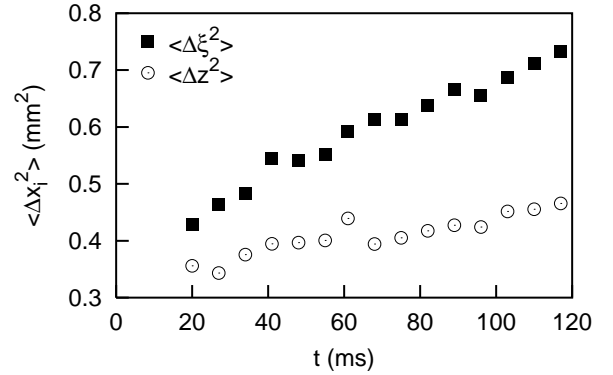


FIG. 6. Atomic mean square displacement as a function of time. The data correspond to a laser detuning of -62.35 MHz and an intensity per lattice beam of 3.2 mW/cm².

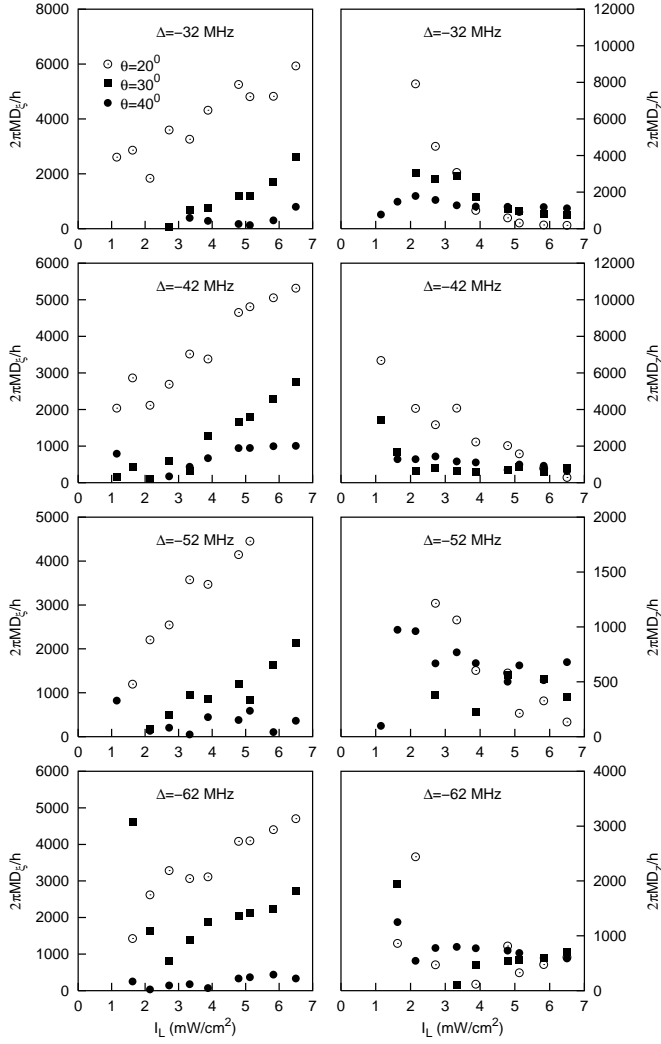


FIG. 7. Experimental results for the spatial diffusion coefficients in the ξ and z -directions as a function of the laser intensity per lattice beam for different values of the lattice detuning and different lattice angles θ .

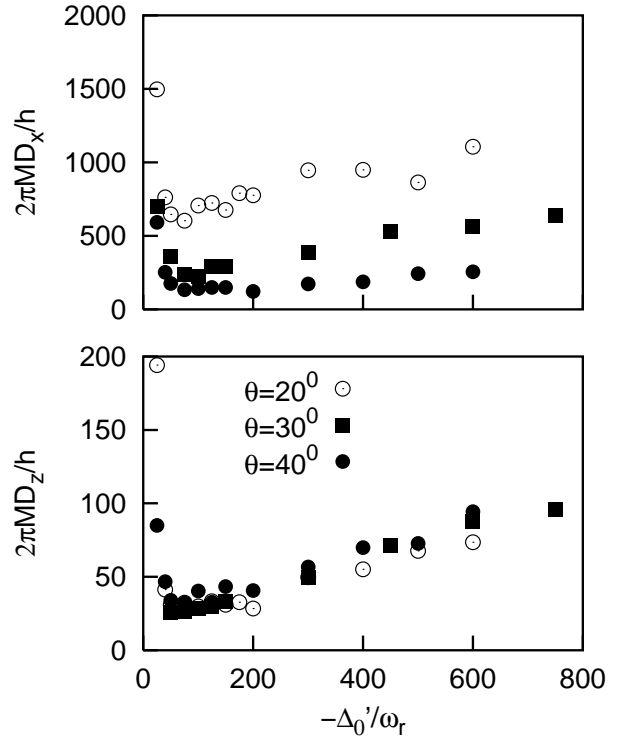


FIG. 8. Numerical results for the spatial diffusion coefficient in the x and z -directions as a function of the light shift per beam at fixed lattice beam detuning ($\Delta = -3\Gamma$, with $\Gamma/2\pi = 5.9$ MHz for ^{85}Rb), i.e. as a function of the lattice beams intensity. The different data sets correspond to different lattice angles θ .